Chapter 2

Experimental Section

2.1. Sample description and preparation

In this thesis, various zeolitic materials have been used. Mordenite was the main focus of the work, while the other zeolites (zeolite A and Faujasite (zeolite X and zeolite Y)) were used for comparison. All the samples used are summarized in Table 1.

Table 1. Summary of all samples used.

Mordenite	Na-Mordenite H-Mordenite Li-Mordenite K-Mordenite Cs-Mordenite Li/Ag-Mordenite Ag-Mordenite Na- Mordenite1%F Li- Mordenite1%F Li/Ag- Mordenite1%F H-Mordenite1%F Na- Mordenite10%F H- Mordenite10%F
Zeolite A	Na/Ag(0.01M)-A Na/Ag(1M)-A
Zeolites X and Y	NaX NaY

In order to understand how zeolites behave in the different processes studied, a structural description of each zeolite is presented below.

2.1.1 Sample description

2.1.1.1. Mordenite

Mordenite is basically a natural mineral, but it can also be synthesized.[1] In the Mordenite framework type, units of four 5-rings are joined to one another via common edges to form chains. Mirror images of these chains are connected via oxygen bridges to form corrugated sheets. These sheets, displaced by half a translation in c, are then connected to one another to form 12-and-8-rings along the corrugations. The lining of the 12-ring channels contains 8-rings, but the 8-ring openings in the adjacent 12-ring channels are displaced, so there is only very limited access from one channel to the next. Consequently the channel system is effectively one dimensional.

Figure 1 shows the Periodic Building Unit (PBU), which is composed of T12 units. Neighbouring PBUs, related by a lateral shift of ½ *b* axes, are connected along the *a* axes.

Cations can be located in different parts of the zeolite channels, which have different roles in the adsorption and catalytic processes. The figure below shows the position of the cationic sites in the mordenite structure according to several studies.[2,3] It seems that half of the Na^+ ions are located in the midle of the compressed channels (site I), while the other half of the total Na^+ cations are located mainly at sites IV and VI (Figure 2).

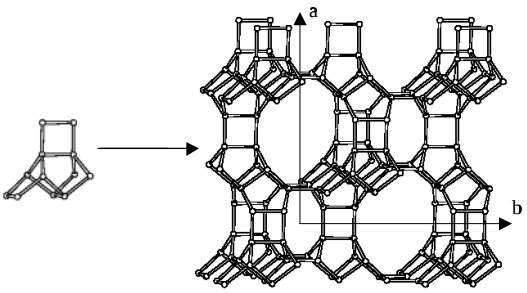

Figure 1. Mordenite's PBU, formed of T12 units (left) and the cell content seen along [001] in perspective view (right).

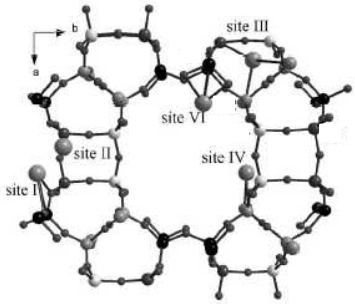

Figure 2. Representation of extra-framework cation sites I, II, III, IV and VI in mordenite

The structure of mordenite is characterized by relatively high silica content, which gives it high thermal stability. Mordenite is also formed of 5-membered rings, which are thought to enhance the acid strength of the material.[4,5] It is the combination of these properties that makes it suitable for such industrial processes as cracking and isomerisation of hydrocarbons,[6] and separation processes.[7] Actually, Tanabe and Hölderich reported that mordenite is used as a catalyst in seven industrial processes.[8]

2.1.1.2. Zeolite A

This zeolite is also known as LTA and is one of the most commonly used zeolites mainly in cation-exchange (as water softener) and in adsorption.

The LTA framework type is related to a sodalite structure. The Periodic Buiding Unit is the so-called sodalite cage or β-cage (Figure 3). In this case, the sodalite cages in a primitive cubic arrangement are joined via double 4-rings rather than single ones (as in the sodalite structure). This creates an α-cage in the center of the unit cell, and a 3-dimensional, 8-ring channel system. Alternatively, the framework can be described as a primitive cubic arrangement of α-cages joined through single 8-rings (producing a sodalite supercage in the center). This is one of the more open zeolite framework types with a framework density of only 12.9 T-atoms per 1000Å^3.

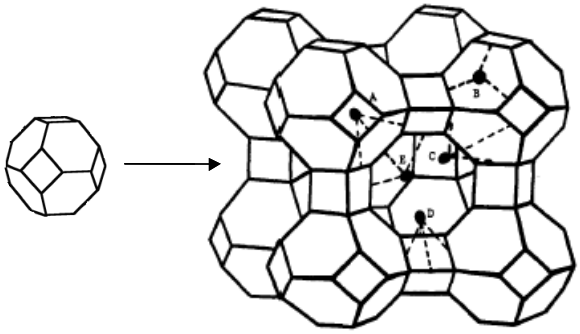

Figure 3. The sodalite cage, T24 unit (left) and unit cell content in perspective view (right)

In this zeolite, with a Si/Al ratio of 1, cations can be located in 4 O-rings (α-cage), in 6 O-rings (α-cage) and in 8 O-rings (β-cages). In the activated sodium

form (i.e. for monovalent cations), eight Na^+ cations are in 6O-rings, three in 8 O-rings and and one in 4 O-rings, while in the calcium form (i.e. for divalent cations) all cations are located in the 6 O-rings.

This zeolite is mainly used as a water softener since it can easily exchange its sodium ions for calcium and magnesium ions.[9]

2.1.1.3. Faujasite

Faujasite is a natural zeolite, while zeolites X and Y are synthetic. Zeolite X is characterized by lower Si/Al ratios (between 1 and 1.5) than zeolite Y (between 1.5 and 3).

Also in this case, the PBU is the β-sodalite cage. The cages are arranged in the same way as the carbon atoms in the diamond, and are joined to one another via double 6-rings. This creates the so-called supercage with four, tetrahedrically-oriented, 12-ring pore openings, and a 3-dimensional channel system (Figure 4).

The combination of large void volume, a 12-ring pore opening and a 3-dimensional channel system makes them ideal for many catalytic applications such as catalytic cracking and hydrocracking, and also separation processes.[10]

For faujasite-type zeolites, the location of cations is well known.[11,12] Thus, in zeolite X with a Si/Al ratio of 1, there are 96 monovalent cations (M^+) per unit cell, $S_{I'}$ and S_{II} are fully occupied by 32 M^+ cations each, and the remaining 32 M^+ are equally distributed between sites S_{III} and $S_{III'}$.

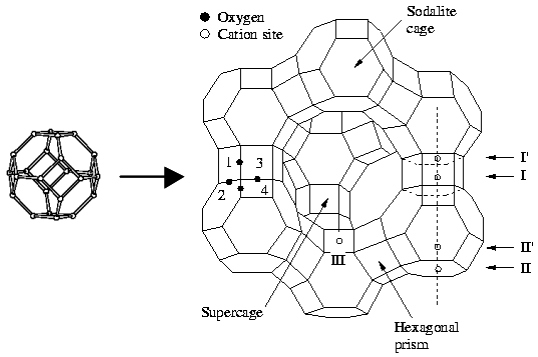

Figure 4. PBU in FAU structure (left) and sodalite cage (right)

2.1.2. Sample preparation

Mordenite, zeolite A and zeolites X and Y were used as starting materials.

Mordenite was purchased from Zeolyst in its sodium form (named as M or MOR through the text). Its chemical composition was SiO_2/Al_2O_3 with a mole ratio of 13 and a Na_2O weight % of 6.6.

Zeolite A was purchased from Prolabo as hydrated binderless pellets with a chemical composition of 1 Na_2O : 1 Al_2O_3 : 2 ± 0.1 SiO_2 : xH_2O.

Zeolite NaY, with a Si/Al ratio of 2.56 was synthesized at the Institute of Industrial Chemistry of Warsaw University while NaX zeolite with a Si/Al ratio of 1.31 was synthesized at the Institute of Chemical Technology of the Jagellonian University in Krakow.

These zeolites were chemically modified so that their properties would be better for the different applications. These chemical modifications are described below:

2.1.2.1. Cationic exchange

The exchange was done with:

a. Alkaline metal salts. High concentrations (2.2 M) of LiCl, KCl and CsCl salts were used. The cation exchange process was repeated several times depending on the cationic exchange properties of the zeolite used. Using this procedure we obtained LiMOR, KMOR and CsMOR and LiA samples.

b. Transition metal salts. In this case, the cationic exchange was done using 0.01 and 1 M concentrations of $AgNO_3$ solution. With this procedure, Na/Ag(1M)-A, Na/Ag(0.01M)-A and Na/AgMOR samples were obtained. The number in brackets, in this case, refers to the concentration of $AgNO_3$ used in the cation exchange.

c. NH_4Cl solution. Cation exchange with NH_4^+ is generally used when the protonic form of a zeolite is required. From the alkaline form, in which the zeolite is generally found, we obtain the NH_4^+-zeolite by exchange, which becomes H-zeolite after calcining at high temperatures. HMOR (or also called HM in some cases) was obtained in this way.

2.1.2.2. Anionic exchange

This exchange was carried out in accordance with the procedure described elsewhere.[13,14] In order to introduce fluorine atoms into the zeolite structure, different concentrations of NH_4F were used. All the fluorine in solution was assumed to have been involved in the attack and NH_4F concentrations were calculated in order to achieve a specific % of F per gram of zeolite. The treatment was made at room temperature and with the protonic form of the zeolite (H-zeolite). Two mordenite-based samples were obtained using this procedure, HM1F and HM10F: the former containing a maximum of 1% in

weight of F atoms per 100 g of zeolite, and the second one containing no more than 10% of F atoms.

Then NaM1F, LiM1F, LiAgM10F and NaM10F were obtained from HM1F and HM10F samples after cation exchanging their ammonium form with NaCl, LiCl and $AgNO_3$ salts, as described above. The ammonium form was obtained by cation exchang of HM1F and HM10F samples with NH_4Cl.

2.1.2.3. Formation of clusters by applying temperature

Different temperatures (between 623 K and 723 K) were applied under vacuum to silver containing zeolites (Ag-A and AgMOR) prepared by cationic exchange with $AgNO_3$ solution as described above, in an attempt to form silver clusters (Ag_m^{n+}) within the zeolite structure. Throughout the procedure, the samples were protected from light in order to prevent silver cations from being reduced to silver atoms.

2.2. Sample characterization

Typical characterization methods were used to characterize the various samples. Basically, most of them are related to surface characterization.

2.2.1. Determination of surface area by N_2 physisorption

N_2 physisorption is one of the oldest techniques in surface characterization. Continued addition of nitrogen gas molecules at 77 K after the monolayer formation leads to the gradual stacking of multiple layers (or multilayers) on top

of each other. As the equilibrium adsorbate pressures approach saturation, the pores become completely filled with adsorbate.

On the basis of the well-known Brunauer, Emmett and Teller (B.E.T.) theory, one can estimate the sample's surface area from the monolayer volume (V_m):

$$V/V_m = c(p/p_o)/[(1-p/p_o)(1-(1-c))(p/p_o)]$$

where V is the volume of gas (STP conditions) adsorbed, V_m is the volume of the gas (STP conditions) adsorbed in the monolayer and p_o is the vapour pressure above the macroscopically thick layer of the pure liquid on the surface. The quantity c approximates to $\exp -(\Delta H_d - H_{vap})/RT$, in which the ΔH_d is the enthalpy of adsorption on the first adsorbed layer and H_{vap} is the heat of vaporisation.

For these measurements we used a Micromeritics ASAP 2000 apparatus. Samples were first activated in vacuum at temperatures between 573 and 623 K.

2.2.2. X-ray diffraction (XRD)

X-ray diffraction is widely used to identify bulk phases and to estimate particle sizes.[15] X-rays have wavelengths in the Å range, which are sufficiently energetic to penetrate solids and well suited to probe their internal structure.

This technique allows us to derive lattice spacings, d, by measuring the 2θ angles under which constructively interfering X-rays, with wave lengh, λ, leave the crystal using the known Bragg Brentano relation:

$$n\lambda = 2 d \sin\theta$$

Additionally, the Scherrer formula relates crystal size to line width:

$$\langle L \rangle = K\lambda / \beta \cos \theta$$

where β is the peak width, corrected respect to the instrumental error, and K is a constant. The linear dimension $\langle L \rangle$ is the volume average thickness of the crystallites, measured normal to the reflecting planes.

In recent years, besides conventional XRD mesurements, high-temperature X-ray diffraction has been increasingly used because it makes possible to directly observe the evolution of structure as a function of the heat treatment.

Conventional powder X-ray diffraction patterns of the samples were obtained with a Siemens D5000 diffractometer (Bragg-Brentano parafocusing geometry and vertical θ-θ goniometer) fitted with a curved graphite diffracted-beam monochromator, incident and diffracted-beam Soller slits, a 0.006º receiving slit and scintillation counter as a detector. The data were collected from 2θ values between 5º and 75º with an angular step of 0.05º at 3s per step and sample rotation. $Cu_{K\alpha}$ (1.542 Å) radiation was obtained from a copper X-ray tube operated at 40kV and 30mA.

High temperature XRD measurements were obtained using a temperature chamber equipped with an Anton-Paar HTK10 platinum ribbon heating stage and connected to a vacuum pump. A Braun position sensitive detector (PSD) was used and the measuring time per degree was 6 sec. A static argon-atmosphere was used throughout the measurement.

The crystalline phases were identified using the Joint Committee on Powder Diffraction Standards (JCPDS) files. From the diffraction patterns, the deconvolutions, cell parameters and cell volumes were calculated using a matching profile with TOPAS 2.1 software (Bruker AXS), in which the instrument error is corrected.

2.2.3. Magic angle spinning nuclear magnetic resonance (MAS NMR)

Since nuclear magnetic resonance (NMR) was discovered, it has emerged as one of the most powerful tools in research for characterising structure, since the observation of the transition frequency measured in the NMR spectrum for an atomic nucleus is a very sensitive probe of its environment.

Since high resolution solid-state NMR was first applied to zeolites in 1979,[16] many authors have worked in this field and contributed to the results and literature available.[17-20]

High-resolution solid NMR spectra can be achieved when line broadening phenomena due to dipolar coupling, chemical shift anisotropy and quadrupolar interaction are removed or reduced. This can be done by Dipolar Decoupling (DD), Multiple Pulse Sequences (MPS), and Magic Angle Spinning (MAS). This last technique, discovered by Andrew et al.[21] and Lowe,[22] is now the one that is most commonly used because line broadenings due to dipolar interactions and chemical shift anisotropy can be reduced to their isotropic values by rotating the sample quickly about an axis inclined at the angle =54º44' (magic angle spinning). MAS NMR can reduce, but not fully remove, quadrupolar line broadenings, for which other techniques are required.

In order to achieve optimum line narrowing and a sufficient signal-to-noise ratio in the solid state NMR spectra, the experimental procedures described above may be used in combination. However, in zeolites, none or only a few hydrogen atoms are present, so Cross Polarization is not an effective technique, and dipolar proton decoupling is not always necessary. Thus, application of MAS is sufficient to remove the chemical shift anisotropy and any small dipolar interaction, and to narrow quadrupolar broadened lines.

All three basic atomic nuclei of framework zeolites can be detected by NMR measurements by its naturally isotopes ^{29}Si, ^{27}Al and ^{17}O. Most elements acting as charge-balancing cations in zeolites also have isotopes that are suitable for NMR experiments (^{7}Li, ^{23}Na, ^{133}Cs, ^{139}La, and ^{205}Tl). Finally, high-resolution solid-state ^{1}H NMR plays an important role in investigating zeolites.

In our case, in order to obtain ^{29}Si NMR and^{27}Al NMR, the MAS technique is mostly sufficient to obtain highly resolved spectra of zeolites. The local environment of the SiO_4 tetrahedra can be derived from the chemical data shift, since it will depend on whether there are 0, 1, 2, 3 or 4 silicon atoms in the four surrounding tetrahedral sites. For Si(0Al,4Si) chemical shifts are expected to be between –105 and –120 ppm; for Si(1Al,3Si) between –95 and 105 ppm; for Si(2Al,2Si) between –90 and –100 ppm; for Si(3Al,1Si) between –90 and –95 ppm; and for Si(4Al,0Si) between –80 and –90 ppm. ^{27}Al NMR spectra of zeolites, however, are generally simpler since, according to Lowenstein's rule, only one environment is possible: $Al(OSi)_4$. Consequently a single narrow peak is observed in the ^{27}Al MAS NMR spectra of zeolites with a typical chemical shift of about 60 ppm (from aqueous $Al(NO_3)_3$ solution) and a non framework aluminium, which is typically an octahedral AlO_6 coordination gives rise to signals at about 0 ppm.[23]

For ^{1}H NMR, the MAS technique was also used. The Brönsted acidic strength depends on the polarisation of the OH bond and therefore on the electronic environment of H, which is determined by its screening constant. Bonardet et al. [23] suggested to use OH chemical-shift as a measure of the Bronsted acidity while other authors use probe molecules.[24] In our case, we use the ^{1}H NMR chemical shift in order to detect changes in Brönsted acidity.

Spectra were obtained at a frequency of 400 MHz by spinning at 5 kHz. The pulse duration was 2 μs and the delay time was 5 seconds. The chemical shift references for aluminum and silicium were high purity octahedral hexahydrated

aluminum chloride $AlCl_3 \cdot 6H_2O$ and silicon nitride Si_3N_4, respectively. In the case of ^1H MAS NMR, TMSP (trimethyl silyl-3-propionic acid 4-2,2,3,3 sodium salt) was used as a reference. All spectra were obtained on a Mercury 400 MHz apparatus.

2.2.4. Fourier transform infra red spectroscopy (FTIR)

The IR technique is one of the oldest instrumental techniques used to study the surface in heterogeneous catalysis including zeolites. Nowadays it is one of the most commonly used surface characterization tools basically because of its low cost and simplicity.

Infrared spectroscopy is extremely valuable for investigating powder samples. It gives direct information about the surface or about the adsorbed species. Mid- and far IR spectra of zeolites are generally used for investigating their framework and cation properties, respectively. However, it gives rather poor information about the acidity of surface hydroxyl groups, which are of great importance for the surface properties.[25] These problems are solved by using probe molecules, which interact with the surface and the alteration of the spectral features as a result of adsorption can provide indirect information about properties, location, and concentration of the surface sites among other things. Several factors must be taken into account when probe molecules are chosen.[26] For example, adsorption complexes should be stable enough to allow characterization; the probe molecules should have spectral parameters that are sensitive to the state of the sites on which they are adsorbed; the informative absorption bands on the surface should be in regions in which the sample is transparent; and the extinction coefficients of their informative bands must be high, otherwise the molecules should not cause any chemical modifications of the surface and be small enough to prevent steric hindrance.

In our case, the experiments were performed on a FTIR Nicolet apparatus in the range 4000-400 cm^{-1}, and the spectra were registered after one hundred scans in transmission mode with a resolution of 4 cm^{-1}. The detector used was KBr deuterated tryglycine sulphate detector (DGTS).

The IR cell (Figure 5) used allows their use on sorption and reaction studies in high vacuum conditions, in which sample handling (activation, adsorption, reaction, and desorption) can be performed in situ.

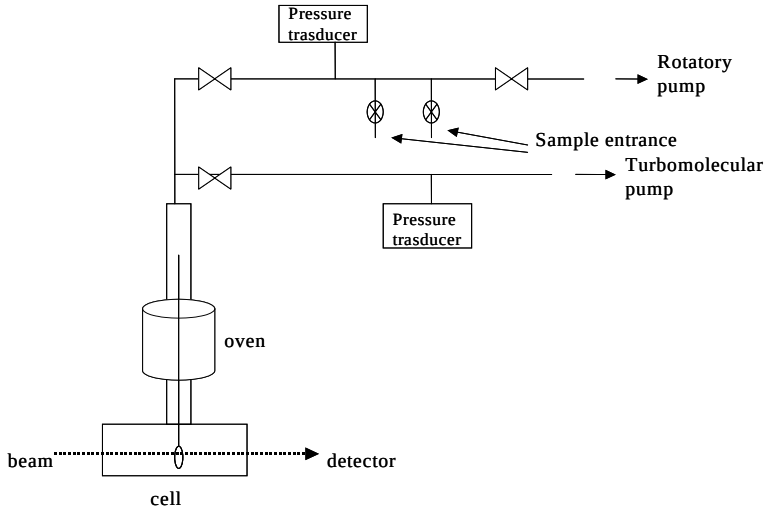

Figure 5. Scheme of an adsorption/desorption in situ IR cell.

Several probe molecules were used in the adsorption/desorption experiments. For example, various nitriles such as acetonitrile (AN), propionitrile (PrN), isobutylonitrile (IBN), pivalonitrile (PN), benzonitrile (BN) and o-toluonitrile (o-TN). These nitriles had different acidity-basicity properties and steric hindrance, which made it possible to characterize the strength and position of the acidic or basic sites in zeolites.[27-30]

Carbon monoxide (CO) was also used as a probe molecule because of its non-reactive adsorption. In this case the oxidation and the coordination states of the metal ions can be determined by the spectral behaviour, stability, and other characteristics of the carbonyls formed.[31] However, low temperature CO adsorption has increasingly been applied to determine the acid strength of the surface hydroxyl groups.[32-34]

Several Far-IR spectra were also taken on a Nicolet Magna 750 in the region 600-50 cm^{-1} using a Polietilene DTGS as a detector.

2.2.5. Ultraviolet-visible spectroscopy (UV-Vis)

UV/VIS spectroscopy is a non-destructive technique for determining the chemical species of a material. A light beam of a certain wavelength range interacts with the sample and the intensity of the transmitted or reflected signal is recorded as a function of the wavelength. Because of the interaction with the sample, at certain frequencies the light is absorbed resulting in absorption peaks in the spectrum. The absorption frequencies are specific for certain chemical compounds and associated with electron transitions in the material. The chemical composition of the sample can therefore be determined by analysing the spectrum using standards that allow quantitative measurement.

The basis of this theory is the Lamber-Beer law:

$$A=ebc$$

where A is absorbance, e is the molar absorbtivity (L mol^{-1} cm^{-1}), b is the path length of the sample (cm) and c is the concentration of the compound in solution (L^{-1}).

In our case, a Shimadzu UV-2101 UPC Diffuse Reflectance UV/Vis apparatus with integrating sphere was used. Spectra were recorded at room temperature in the range 200 nm to 800 nm.

2.2.6. Temperature programmed desorption (TPD)

Temperature programmed desorption relates some characteristic properties of a sample to its temperature in the course of a temperature-programmed heating. In TPD studies a solid that has previously been equilibrated with an adsorbing gas in well-defined conditions is submited to a programme temperature rise and the amount of gas desorbed is continuously monitored.

In our case the apparatus used is a TPD/R/O 1100 Thermo Finnigan equipped with a temperature-programmable oven, a thermal conductivity detector (TCD) and a PFEIFFER GSD 301 02 mass spectrometry detector.

For the pre-treatment, samples were activated in situ by flowing Ar at increasing temperature. Afterwards, the corresponding probe molecule gas was adsorbed at 313 K and desorbed by flowing He 20 cm^3/min. The conditions used for each sample are specified in the corresponding section. The gases used for sample characterization were NH_3 in He, CO_2 and acetonitrile (CH_3CN).

In some cases, a more exhaustive characterisation was necessary, for which the following techniques were used.

2.2.7. X-ray fluorescence (XRF) spectroscopy

An electron microscope offers additional possibilities for analysing the sample. Emitted X-rays are characteristic of an element and make possible to determine the chemical composition of a particular part of a sample.

In our case, X-ray fluorescence was used to determine the atomic distribution maps and the Si/Al ratio of several samples. Experiments were performed on a scanning electron microscope, JEOL JSM6400, operating at accelerating voltage of 15 kV and work distances of 15 mm. All samples were covered with a graphite layer. Accumulating time for mapping experiments was around 120 seconds.

2.2.8. Elementary analysis

Atomic absorption spectroscopy (AAS) and induced coupled plasma (ICP), both based on the Planck equation, are considered to be two of the best techniques for zeolite elementary analysis.

The elementary analysis of zeolites for their major and minor components requires a sample preparation approach that will dissolve a wide variety of elements without volatilisation or precipitation losses. One of the most commonly used procedures is to perform a sample digestion in cold hydrofluoric acid. Due to the ability of HF to attack glass containers, the whole pre-treatment process was performed on polypropilene vessels.

The method to be used depends on the sample, the matrix sample, the desired analysis accuracy and also on the time and funds available.

We used ICP for Al, K, and Ca determination and AAS for Li and Na determination.

2.2.9. Cation exchange capacity (CEC)

Cation exchange capacity gives information about the number of exchangeable cations, which can be replaced more or less easily with other cations without affecting the aluminosilicate framework. The magnitude of such cation

exchange in a given zeolite is known as its cation-exchange capacity (CEC) and is commonly measured in terms of moles or equivalents of exchangeable cations per gram of zeolite.

Several methods have been described in the literature for CEC determination. In our case, the CEC of several mordenite samples was determined in a similar way to that proposed by Bergaya et al.[35] First, mordenite samples were exchanged with an aqueous solution of $CuSO_4$ for 6 h at room temperature. Then, the samples were centrifuged and washed with distilled water several times. The amount of Cu^{2+} exchanged was determined by UV-visible spectroscopy at 809 nm. The CEC in meq/100g of zeolite was calculated as the difference in Cu^{2+} concentration between the starting solution and the final solution obtained after the cationic exchange.

2.3. Adsorption and catalytic experiments

2.3.1. Adsorption experiments

In order to test the adsorption properties of the adsorbants, we measured the adsorption isotherms of the isolated adsorbates, which are high purity N_2 and O_2. The adsorption properties measured were:

1. Sorption capacity of each gas (N_2 and O_2), expressed as the volume in cm^3 of gas adsorbed per gram of sample before activation.
2. Sorption N_2/O_2 selectivity, which was calculated as the ratio between the volume of N_2 adsorbed and the O_2 adsorbed volume at a given pressure.

Adsorption isotherms were measured using a static volumetric system Micromeritics ASAP-2010. The gases used were high purity (99.999%) N_2 and O_2. Both gases were supplied by Carburos Metálicos.

Experiments were made using 0.20-0.30 g. of sample. The sample was contained in a quartz cup. Due to the fact that small amounts of molecular water inside the framework of the aluminosilicates seriously affect their adsorption capacity,[36] samples were activated with temperature in vacuum using a turbomolecular vacuum pump to a pressure lower than 1μmHg before the adsorption measurements were made. Adsorption isotherms were measured at 298 K in the pressure range 0.05 and 760 mmHg.

2.3.2. Catalytic experiments

As stated above, the aim of these catalytic tests was to check the acidity of some samples after specific modifications had been made.

The reaction studied was the acid catalysed isomerisation of styrene oxide (SO) to give the corresponding phenylacetaldehyde (PA).

Isomerisation reactions were carried out in liquid phase using batch reactors heated by conventional methods and also by microwaves.

The experiments using batch reactors with conventional heating were carried out in an oil bath and using a contact thermometer.

The experiments heated using microwaves were performed in a Milestone ETHOS-TOUCH CONTROL equipped with a temperature controller at a work frequency of 2.45 GHz and using closed vessels. The main advantages of using this technology are the faster preparation rate and the high yields and purity of the products obtained. However, microwaves have not been practically used in catalysis until now. The closed vessels provide a clean

environment for the sample during processing and prevent the loss of volatile species, even when the materials are processed at temperatures well above the normal boiling point of the mixture.

The catalytic experiments were performed using 0.04 g of catalyst, 25 ml of solvent (n-hexane or methanol) and 0.3 ml of reactant (SO or PA). PA was used as a reactant for purposes of comparison, as we will see in the results and discussion section. In all cases, catalysts and solvents were first activated using the appropriate procedures.

The reaction products were analysed by gas chromatography (GC) on a Shimadzu GC-2010 instrument equipped with a 30 m capillary column RTX-5 coated with phenylmethylsilicon and a FID detector.

Conversion was defined by the following equations:

$$[[\text{area PA/area SO}]_{\text{after reaction}}-[\text{area PA/area SO}]_{\text{before reaction}}]\ g\ cat^{-1}$$

$$[[\text{area MPE/area SO}]_{\text{after reaction}}]\ g\ cat^{-1}.$$

where PA means phenylacetaldehyde; SO, styrene oxide and MPE, 2-methoxy-2-phenylethanol.

2.4. References

[1] Barrer, R. M. *J. Chem. Soc.* **1948**, 2158.

[2] Maurin, G.; Bell, R. G.; Devautour, S.; Henn, F.; Giuntini, J. C. *J. Phys. Chem. B* **2004**, 108, 3739.

[3] Devautour, S.; Abdoulaye, A.; Giuntini, J. C.; Henn, F. *J. Phys. Chem. B* **2001**, 105, 9297.

[4] Nagy, J. B.; Bodart, P.; Hannus, I.; Kiricsi, I. *Synthesis, characterization and use of zeolitic microporous materials*, DecaGen Ltd: Szeged (Hungary), 1998.

[5] Van Bokhoven, J. A.; Tromp, M.; Koningsberger, D. C.; Miller, J. T.; Pieterse, J. A. Z.; Lercher, J. A.; Williams, B. A.; Kung, H. H. *J. Catal.* **2001**, 202, 129

[6] Moreau, F.; Ayrault, P.; Gnep, N. S.; Lacombe, S.; Merlen, E.; Guisnet, M. *Microp. Mesop. Mat.* **2002**, *51*, 211.

[7] Méthivier, A.; Separation of Paraxylene by Adsorption. In *Zeolites for cleaner technologies* Guisnet M.; Gilson, J. P.; Eds.; Imperial College Press: London, Catalytic Science Series, Vol 3, 2002, p. 209.

[8] Tanabe, K.; Hölderich, W. F. *Appl. Catal. A- Gen.*, **1999**, 181, 399.

[9] Rees, L. V. C.; Ion Exchange and Detergent Building. In *Zeolites as Catalysts, Sorbents and Detergents Builders* Karge, H. G.; Weitkamp, J. Eds.; Elsevier: Amsterdam, 1989.

[10] Coe, C. G. Structural Effects on the Adsorptive Properties of Molecular Sieves for Air Separation. In *Access in Nanoporous Materials, Procedings of a Symposium on Access in Nanoporous Materials*. East Lansing, Michigan, 1995, p. 213.

[11] Breck, D. W. *Zeolite Molecular Sieves: Structure, Chemistry and Use*, John Wiley: London, 1974, p. 97.

[12] Plévert, J.; DiRenzo, F.; Fajula, F.; Chiari, G. *J. Phys. Chem. B* **1997**, 101, 10340.

[13] Kowalak, S.; Khodakov, A. Y.; Kustov, L. M.; Kazanky, V. B. *J. Chem. Soc. Faraday Trans.* **1995**, 91, 385.

[14] Becker, K. A.; Kowalak, S. *J. Chem.Soc., Faraday Trans I* **1985**, 81, 1161.

[15] Cohen, J. B.; Schwartz, L. H. *Diffraction from Materials*, Academic Press, New York, 1977.

[16] Engelhardt, G.; Kunath, D.; Mägi, M.; Samson, A.; Tarmak, M.; Lippmaa, E. *Preprints of the Workshop "Adsorption of Hydrocarbons in Zeolites"*, Berlin-Adlershorf, 1979.

[17] Engelhardt, G.; Michel, D. *High –Resolution Solid-State NMR of Silicates and Zeolites*, John Wiley and Sons: Chichester, 1987.

[18] Stöcker, M. Review on recent NMR Results. In *Advanced Zeolite Science and Applications* Jansen, J. C.; Stöcker, M.; Karge, H. G.; Weitkamp, J. Eds.; Elsevier: Amsterdam, 1994 , vol 85, p. 429.

[19] Srikanth, K.; Schurko, R. W.; Hung, I.; Ramamoorthy, A. *Mater. Sci. Tech-Lond.* **2003**, 19 (9), 1191.

[20] Pruski, M.; Amoureux, J. P.; Fernandez, C. Progress in high resolution solid state NMR of quadrupolar nuclei. Applications to porous materials and catalysts. In *Magnetic Resonance in Colloid and Interface Science*, Resing H. A.; Wade, C. G. Eds.; ACS Symposium Series: San Francisco, 1976, vol. 76, p. 107.

[21] Andrew, E. R.; Bradbury, A.; Eades, R.G. *Nature*, **1958**, 182, 1659.

[22] Lowe, I. J. *Phys. Rev. Lett.* **1959**, 2, 285

[23] Bonardet, J. L.; de Menorval, L. C.; Fraissard, J Some applications of high resolution NMR to the study of gas-solid interactions. I. Chemical shift of

nuclei at solid surfaces. II. Chemisorption of hydrogen on oxide-supported platinum. In *Magnetic Resonance in Colloid and Interface Science*, Resing H. A.; Wade, C. G. Eds.; ACS Symposium Series: San Francisco, 1976, vol. 76, p. 248.

[24] Semmer-Herlédan, V.; Heeribout, L.; Batamack, P.; Dorémieux-Morin, C.; Fraissard, J.; Gola, A.; Benazzi, E. *Microp. Mesop. Mat.* **2000**, 34, 157-169.

[25] Busca, G. *Phys. Chem. Chem. Phys.* **1999**, 1, 723.

[26] Hadjiivanov, K. I.; Vayssilov, G. N., Adv. Catal. **2002**, 47, 309.

[27] Bevilacqua, M.; Busca, G. *Catal. Commun.* **2002**, 3, 497.

[28] Bevilacqua, M.; Gutièrrez Alejandre, A.; Resini, C.; Casagrande, M.; Ramírez, J.; Busca, G. *Phys. Chem. Chem. Phys.* **2002**, 4, 4575.

[29] Bordiga, S.; Turnes Palomino, G.; Pazè, C.; Zecchina, A. *Microp. Mesop. Mat.* **2000**, 34, 67.

[30] Lavalley, J. C. *Catal. Today* **1996**, 27, 377.

[31] Bordiga, S.; Lamberti, C.; Geobaldo, F., Zecchina, A.; Turnes Palomino, G; Otero Areán, C. Langmuir **1995**, 11, 527.

[32] Mauche, M.; Janin, A.; Lavalley, J. C.; Benazzi, F. *Zeolites* **1995**, 15, 507.

[33] Cairon, O.; Chevereau, T.; Lavalley, J. C. *J. Chem. Soc. Faraday Trans.* **1998**, 94, 3039.

[34] Marie, O.; Massiani, P.; Thibault-Starzyk, F. *J. Phys. Chem. B* **2004**, 108, 5073.

[35] Bergaya, F.; Vayer, M. *Appl. Clay Sci.* **1997**, 12, 275.

[36] Hutson, N. D.; Zajic, S. C.; Yang, R. T. *Ind. Eng. Chem. Res.* **2000**, 39, 1775.